Title

Feasibility of atlas-based active bone marrow sparing intensity modulated radiation therapy for cervical cancer

Journal

Radiotherapy and Oncology, 123(2)

ISSN

0167-8140

Authors

Li, Nan
Noticewala, Sonal S
Williamson, Casey W
et al.

Publication Date

2017-05-01

DOI

10.1016/j.radonc.2017.02.017

Peer reviewed

Radiotherapy and Oncology 123 (2017) 325–330

Contents lists available at ScienceDirect

Radiotherapy and Oncology

journal homepage: www.thegreenjournal.com

IMRT in cervical cancer

Feasibility of atlas-based active bone marrow sparing intensity modulated radiation therapy for cervical cancer

Nan Li [a], Sonal S. Noticewala [a], Casey W. Williamson [a], Hanjie Shen [a], Igor Sirak [b], Rafal Tarnawski [c], Umesh Mahantshetty [d], Carl K. Hoh [e], Kevin L. Moore [a], Loren K. Mell [a,*]

[a] Department of Radiation Medicine and Applied Sciences, University of California San Diego, La Jolla, United States; [b] Department of Oncology and Radiotherapy, University Hospital, Hradec Kralove, Czech Republic; [c] Clinic of Radiotherapy, Maria Skłodowska-Curie Memorial Cancer Center and Institute of Oncology, Gliwice, Poland; [d] Department of Radiation Oncology, Tata Memorial Hospital, Mumbai, India; and [e] Department of Radiology, Division of Nuclear Medicine, University of California San Diego, La Jolla, United States

ARTICLE INFO

Article history:
Received 4 October 2016
Received in revised form 30 January 2017
Accepted 25 February 2017

Keywords:
^{18}F-FDG PET/CT
Atlas-based
Active bone marrow
Radiotherapy planning

ABSTRACT

Background: To test the hypothesis that atlas-based active bone marrow (ABM)-sparing intensity modulated radiation therapy (IMRT) yields similar dosimetric results compared to custom ABM-sparing IMRT for cervical cancer patients.

Methods: We sampled 62 cervical cancer patients with pre-treatment FDG-PET/CT in training (n = 32) or test (n = 30) sets. ABM was defined as the subvolume of the pelvic bone marrow (PBM) with standardized uptake value (SUV) above the mean on the average FDG-PET image (ABM_{Atlas}) vs. the individual's PET (ABM_{Custom}). Both were deformed to the planning CT. Overlap between the two subvolumes was measured using the Dice coefficient. Three IMRT plans designed to spare PBM, ABM_{Atlas}, or ABM_{Custom} were compared for 30 test patients. Dosimetric parameters were used to evaluate plan quality.

Results: ABM_{Atlas} and ABM_{Custom} volumes were not significantly different (p = 0.90), with a mean Dice coefficient of 0.75, indicating good agreement. Compared to IMRT plans designed to spare PBM and ABM_{Custom}, ABM_{Atlas}-sparing IMRT plans achieved excellent target coverage and normal tissue sparing, without reducing dose to ABM_{Custom} (mean ABM_{Custom} dose 29.4 Gy vs. 27.1 Gy vs. 26.9 Gy, respectively; p = 0.10); however, PTV coverage and bowel sparing were slightly reduced.

Conclusions: Atlas-based ABM sparing IMRT is clinically feasible and may obviate the need for customized ABM-sparing as a strategy to reduce hematologic toxicity.

 Radiotherapy and Oncology 123 (2017) 325–330

Concurrent chemoradiotherapy (CRT) is standard treatment for women with locoregionally advanced cervical cancer [1–5]. However, hematologic toxicity (HT) is a significant clinical problem that limits the intensity of CRT, which can lead to chemotherapy dose reductions and/or treatment breaks, potentially compromising patient outcomes [6–8]. Clinical studies have shown that increased radiation dose and volume of irradiated pelvic bone marrow (PBM) are associated with increased risk of HT, suggesting that techniques designed to limit PBM irradiation could reduce toxicity [9,10]. Intensity modulated radiation therapy (IMRT) is a technology that can reduce toxicity by decreasing dose to normal tissues, without compromising tumor control. However, current IMRT plans are constrained by the large PBM volume to avoid, as defined by computed tomography (CT) [11,12].

Previous studies have suggested that refining IMRT plans to spare hematopoietically "active" bone marrow (ABM) subregions could be an effective strategy to reduce HT [13–18]. Functional imaging using [^{18}F] fluoro-2-deoxy-2-D-glucose (FDG) and 3′-deoxy-3′-[^{18}F] fluorothymidine (FLT) positron emission tomography/CT (PET/CT) are potential methods for identifying metabolic or proliferative subregions within PBM, in order to use these subregions in IMRT planning as avoidance structures. Although studies have found that incorporating functional imaging with IMRT planning is likely to be effective [15–19], this approach remains investigational. Moreover, functional imaging is expensive and not universally available.

To address this problem, McGuire et al. [20] proposed a method to identify ABM using FLT-PET in 18 subjects. However, their study did not investigate the dosimetric impact of atlas-based ABM for IMRT planning (obviating personalized functional imaging) relative to customizing the ABM subvolume for each patient (which would require functional imaging in each patient). Therefore, in this study, we sought to test the hypothesis that atlas-based ABM-sparing could yield similar dosimetric results compared to custom ABM-sparing for cervical cancer patients undergoing IMRT.

* Corresponding author at: Department of Radiation Medicine and Applied Sciences, 3855 Health Sciences Drive, MC0843, La Jolla, CA 92093, United States.
E-mail address: lmell@ucsd.edu (L.K. Mell).

http://dx.doi.org/10.1016/j.radonc.2017.02.017
0167-8140/

Materials and methods

Sampling methods

This study was approved by the participating institutions' review boards and is compliant with the Health Insurance Portability and Accountability act. The sample consisted of 62 patients with stage IB-IVA cervical cancer treated on one of two prospective clinical trials investigating IMRT with concurrent chemotherapy; 41 patients were enrolled in a multi-institutional phase II trial (clinicaltrials.gov identifier: NCT01554397) and 21 were enrolled in a single-institution phase I clinical trial (clinicaltrials.gov identifier: NCT1554410). All patients had a pre-treatment FDG-PET/CT and planning (simulation) CT. Patients were randomly separated into training ($N = 32$) and test ($N = 30$) sets for further analysis.

Imaging and segmentation methods

Patients from different institutions underwent FDG-PET/CT scans using different PET/CT scanners. UCSD and CZHK performed FDG-PET/CT scans using a GE Medical Systems Discovery STE model, MSCC using SIEMENS Systems Biograph 128_mCT model, and TATA using PHILIPS Medical Systems GEMINI TF TOF 64 model. The planning CT and FDG-PET/CT scan for each patient were imported into Velocity software (Velocity Medical Solutions, Atlanta, GA) for image processing and analysis.

PBM was contoured on the planning CT and was defined as the L5 vertebral body, os coxae, entire sacrum, coccyx, and proximal femora superior to the level defined by the most caudal point of the ischial tuberosities. As described in previous studies [16,17], the ABM was defined as a subvolume of PBM with standardized uptake values corrected for body weight (SUV) greater than or equal to individuals' mean SUV over the entire PBM volume.

To generate the custom ABM (ABM_{Custom}) for each patient, the individual's FDG-PET/CT scans were deformably registered to the patient's planning CT, optimizing in the region of PBM. The registered PET images were resampled to match the voxel dimensions of the planning CT. The mean SUV of the total PBM on each of the deformed and resampled PET image served as a threshold for ABM_{Custom} segmentation. Lastly, we registered the ABM_{Custom} contour to the patient's simulation CT for IMRT planning.

In order to generate the ABM atlas, an individual with an intermediate-sized PBM volume was selected from the whole sample set to represent the canonical template. Standardization was achieved by deformably registering each individual's FDG-PET/CT to the template planning CT and resampling the registered PET image to match the template CT voxel dimensions. The deformable registration algorithm utilized in Velocity is a modified B-spline method with mutual information-based matching. Subsequently, the mean FDG-PET image was created by averaging the SUV of all 32 standardized PET images. Finally, the ABM atlas was defined on the mean FDG-PET image using values above the mean SUV as a threshold.

Active bone marrow-sparing IMRT planning

To generate the atlas-based ABM (ABM_{Atlas}) for each patient, the mean FDG-PET image was deformed and resampled to the individual's planning CT using deformable registration. The Dice coefficient was used to measure the percentage of overlap of ABM_{Custom} and ABM_{Atlas} for each patient:

$$\text{Dice coefficient} = \frac{2 \cdot N(\text{A} \cap \text{B})}{N(A) + N(B)}$$

where $N(\text{A} \cap \text{B})$ is the number of elements that intersect between set A and set B, $N(A)$ is the number of elements in set A, and $N(B)$ is the number of element in set B [19]. Note that the Dice coefficient is meaningful when the two volumes have approximately similar size.

To compare ABM_{Atlas}-sparing versus ABM_{Custom}-sparing IMRT plans, 3 IMRT plans were generated for each patient. The first (PBM-sparing IMRT plan) included one planning target volume (PTV) and 4 organs at risk (OARs): PBM, bowel, bladder and rectum, in the optimization process. The other two plans, denoted as ABM_{Atlas}-sparing and ABM_{Custom}-sparing plans, used the same objectives and priorities as the PBM-sparing IMRT plan plus an additional avoidance structure for either ABM_{Atlas} or ABM_{Custom}, respectively.

All plans were generated using the Eclipse v13.6 treatment planning system (Varian Medical Systems, Palo Alto, CA) and prescribed as 45.0 Gy in 1.8 Gy daily fractions. We used knowledge-based planning software (RapidPlan®) to set the objectives and priorities for each structure; this method can predict achievable dose–volume histogram (DVH) estimations using a validated model based on patients' specific anatomy and generate patient-specific optimization objectives for automated plan optimization [21,22] (Table 1). We used either static-field IMRT or Volumetric Modulated Arc Therapy (VMAT), depending on the setup of the original protocol plan for that patient. All plans were normalized to cover 95% of PTV volume with 100% of the prescription dose before plan comparison.

All plans generated by the RapidPlan system were reviewed carefully and, when necessary, fine-tuned to make them clinically acceptable. The only notable issue that required refinement was, on occasion, hot spots observed outside of PTV. Standardized re-tuning of the normal tissue objective (increase priority 100–150 and decreased starting distance from target border 10 mm to 2 mm) eliminated these in all cases, and this refinement made negligible changes to other plan quality metrics but ensured a fair comparison between plans.

Statistical methods

For continuous measures we used an independent sample t-test, while for categorical measures we used Fisher's exact test to assess differences between the training and test set for the sample demographic and cancer characteristics. Paired t-test was used to test the null hypothesis of no difference between ABM_{Atlas} and ABM_{Custom} volumes, Dice coefficients, and dose–volume metrics.

Results

Table 2 shows the sample characteristics across the subgroups. The mean age for the whole cohort was 49.3 years old. The training and test set did not differ significantly in age, treating institution status, race, histology, and mean pelvic bone marrow (PBM) volume. However, the groups significantly differed by stage ($p = 0.03$).

Fig. 1 depicts the heat map of the mean ABM atlas generated using standardized FDG-PET images of the 32 training patients. We observed no significant difference between ABM_{Custom} vs. ABM_{Atlas} volumes ($p = 0.9$) (Fig. 2a). The mean volumes of ABM_{Custom} vs. $ABM_{Atlas,}$ as a percentage of PBM, were 44.3% vs. 44.4% for the whole cohort and 43.6% vs. 44.8% for the test subset, respectively. The mean Dice coefficient between ABM_{Custom} and ABM_{Atlas} was 0.75 (standard deviation (SD): 0.055) for all patients and 0.74 (SD: 0.054) for patients in the test subset (Fig. 2b and c) indicating a high proportion of overlap and good agreement between ABM_{Custom} and ABM_{Atlas} volumes.

To analyze the dosimetric effects of ABM_{Atlas}-sparing IMRT planning, we compared the average DVHs (Fig. 3) and mean DVH metrics (Table 3) from the three different plans for 30 test patients.

Table 1
Optimization objective and priority settings for all structures.

Structure	Objectives	Priorities		
		PBM plan	ABM_{Custom} plan	ABM_{Atlas} plan
PTV	D_{max} < 105% of Rx		80	
	$D_{10\%}$ < 103% of Rx		80	
	$D_{99\%}$ > Rx		100	
	D_{min} > 98% of Rx		100	
PBM	D_{max} < Rx		50	
	V_{10} < Model Generated		200	
	V_{20} < Model Generated		200	
	V_{30} < Model Generated		80	
	V_{40} < Model Generated		50	
Bowel	D_{max} < Rx		100	
	V_{30} < Model Generated		80	
	V_{40} < Model Generated		200	
	V_{45} < Model Generated		200	
Bladder	D_{max} < Rx		80	
	V_{20} < Model Generated		50	
	V_{40} < Model Generated		80	
Rectum	D_{max} < Rx		80	
	V_{30} < Model Generated		50	
	V_{40} < Model Generated		80	
ABM_{Custom}	V_{10} < Model Generated	NA	200	NA
	V_{20} < Model Generated	NA	200	NA
	V_{30} < Model Generated	NA	80	NA
	V_{40} < Model Generated	NA	50	NA
ABM_{Atlas}	V_{10} < Model Generated	NA	NA	200
	V_{20} < Model Generated	NA	NA	200
	V_{30} < Model Generated	NA	NA	80
	V_{40} < Model Generated	NA	NA	50

PTV, planning target volume; PBM, pelvic bone marrow; ABM, active bone marrow; Rx, prescription.

Table 2
Sample characteristics.

Characteristic	All	Training Set	Test Set	*p*-Value (Training vs. Test)
Number of patients	62	32	30	
Mean age, years (SD)	49.3 (11.8)	50.8 (12.4)	47.7 (11.2)	0.298#
Age range, years	30–73	30–73	30–68	
Institution, *n* (%)				0.126*
UCSD	36 (58.1)	22 (68.8)	14 (46.7)	
CZHK	13 (21.0)	6 (18.8)	7 (23.3)	
MSCC	9 (14.5)	4 (12.5)	5(16.7)	
TATA	4 (6.5)	0 (0)	4 (13.3)	
Race, *n* (%)				0.209*
Caucasian	37 (59.7)	17 (53.1)	20 (66.7)	
Hispanic	14 (22.6)	9 (28.1)	5 (16.7)	
Asian	8 (12.9)	3 (9.4)	5 (16.7)	
Other	3 (4.8)	3 (9.4)	0 (0.0)	
FIGO stage, *n* (%)				0.030*
IB1	3 (4.8)	1 (3.1)	2 (6.7)	
IB2	9 (14.5)	3 (9.4)	6 (20)	
IIA	1 (1.6)	1 (3.1)	0 (0.0)	
IIB	32 (51.6)	14 (43.8)	18 (60)	
IIIB	16 (25.8)	13 (40.6)	3 (10)	
IVA	1 (1.6)	0 (0.0)	1 (3.3)	
Histology, *n* (%)				1.000*
Squamous	50 (80.6)	26 (81.3)	24 (80)	
Adenocarcinoma	12 (19.4)	6 (18.8)	6 (20)	
Mean PBM volume, cm^3 (SD)	1211.5 (200.5)	1192.8 (184.4)	1231.5 (217.6)	0.452#
PBM volume range, cm^3	876.6–1764	880.9–1496.8	876.6–1764	

SD, sample standard deviation; *n*, number; PBM, pelvic bone marrow; UCSD, University of California San Diego; CZHK, University Hospital Hradec Kralove; MSCC, Marie Sklodowska Cancer Center Gliwice Poland; TATA, Tata Memorial Hospital; FIGO, International Federation of Gynecologic Oncology; #: *p* value from independent sample *t*-test; *: *p* value from Fisher's exact test.

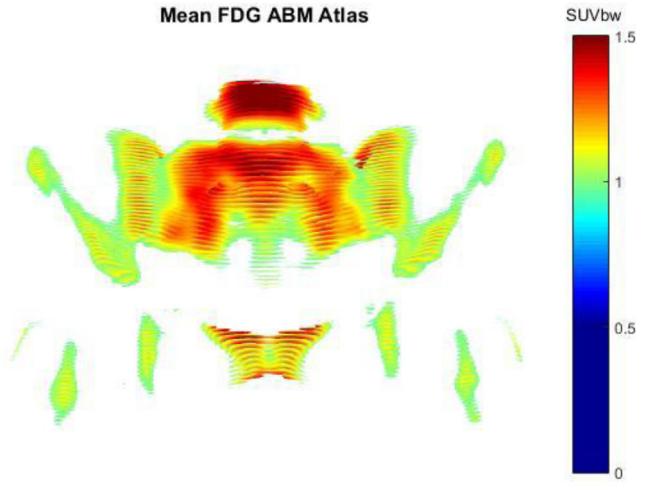

Fig. 1. Heat map of the mean active bone marrow (ABM) atlas generated using standardized FDG-PET images of the 32 training patients.

ABM_{Atlas} plans were not worse than PBM-sparing or ABM_{Custom}-sparing plans with regard to ABM_{Custom} dose; however, PTV coverage and bowel sparing were reduced slightly.

Discussion

In this study, we observed a good agreement between the metabolically active marrow regions defined by an atlas (model) and the customized active marrow defined for each individual based on their pre-treatment FDG-PET/CT. Moreover, we found that atlas-based plans were as effective in reducing dose to active bone marrow as plans customized to avoid those regions. Although this may seem counterintuitive, we speculate that atlas-based ABM-sparing plans are not constrained by reducing dose to outlier subregions, and instead are highly effective at reducing dose to active marrow regions common to most individuals. Altogether, our findings indicate that atlas-based ABM-sparing IMRT is feasible and may obviate the need for custom ABM-sparing approaches as a strategy to reduce hematologic toxicity (HT).

Prior studies indicate that reducing dose to ABM is likely to be an effective method to reduce HT, potentially allowing the delivery of more chemotherapy [9,10,15,23,24]. Normal tissue complication studies have found that decreased dose to the pelvic bone marrow is associated with reduced HT [9,10,23]. Furthermore, pelvic bone marrow dose–volume metrics have been linked to weekly reductions in peripheral blood counts in cervical cancer patients receiving CRT [25]. We have previously shown that radiation to functionally ABM identified by FDG-PET was associated with HT and IMRT can reduce dose to ABM subregions delineated by func-

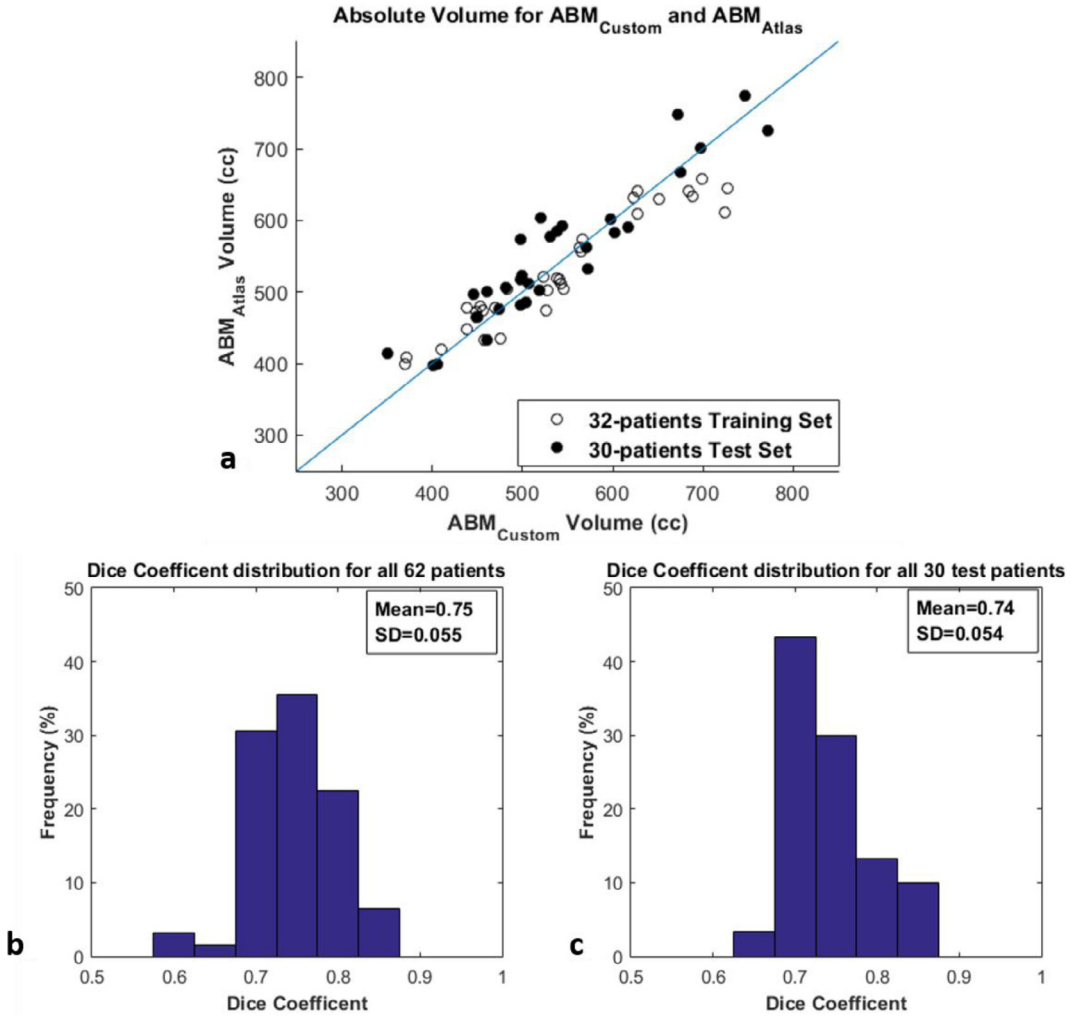

Fig. 2. Absolute volumes and Dice coefficient distributions. (a) ABM_{Custom} and ABM_{Atlas} absolute volumes comparison; (b) Dice Coefficient distribution for all 62 patients with mean (SD) value of 0.75(0.055); (c) Dice Coefficient distribution for 30 test patients with mean (SD) value of 0.74(0.054). PBM, pelvic bone marrow; ABM, active bone marrow.

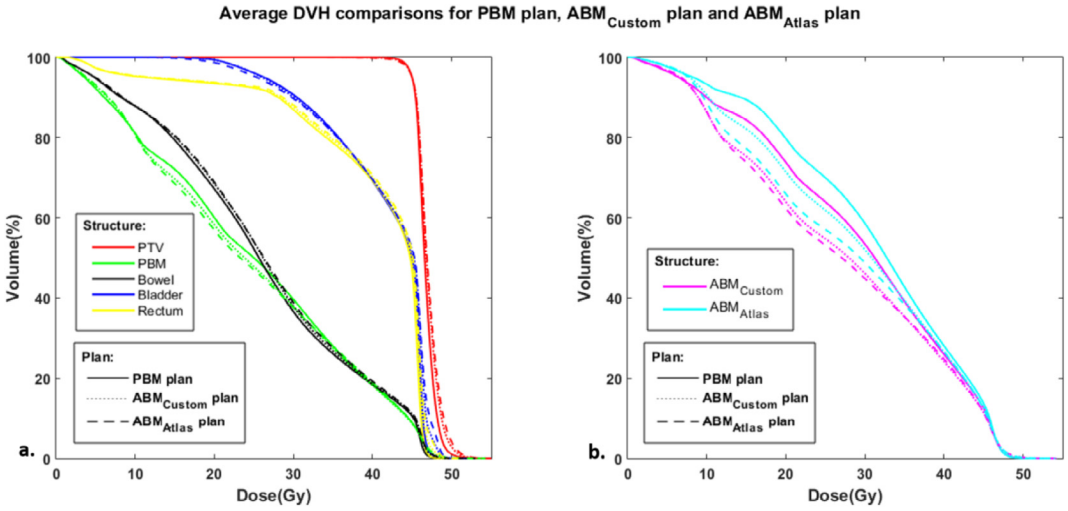

Fig. 3. Average DVH comparison for PBM plan, ABM_{Custom} plan and ABM_{Atlas} plan. (a) DVH comparison for PTV, PBM, bowel, bladder, and rectum. (b) DVH comparison for ABM_{Custom} and ABM_{Atlas}. DVH, dose–volume histogram; PBM, pelvic bone marrow; ABM, active bone marrow; PTV, planning target volume.

Table 3
Comparison of dose–volume metrics.

Structure	Metrics	PBM plan	ABM_{Custom} plan	ABM_{Atlas} plan	p-Value* (ABM_{Custom} vs. ABM_{Atlas} plan)
PBM	V_{10}, % (SD)	81.1 (5.6)	80.8 (5.5)	80.6 (5.3)	0.37
	V_{20}, % (SD)	60.0 (6.3)	58.2 (5.8)	56.9 (5.6)	**<0.01**
	V_{30}, % (SD)	39.6 (5.8)	37.8 (5.4)	37.6 (5.1)	0.44
	V_{40}, % (SD)	18.4 (3.9)	18.2 (3.6)	18.9 (3.4)	**0.02**
	D_{mean}, Gy (SD)	24.9 (1.9)	24.5 (1.8)	24.4 (1.8)	0.17
ABM_{Custom}	V_{10}, % (SD)	89.9 (5.2)	86.3 (5.8)	86.4 (6.3)	0.81
	V_{20}, % (SD)	73.8 (8.0)	63.9 (5.2)	62.3 (6.5)	**0.02**
	V_{30}, % (SD)	53.4 (8.5)	46.1 (5.3)	44.8 (6.2)	**0.03**
	V_{40}, % (SD)	26.0 (6.4)	24.2 (4.9)	24.7 (5.2)	0.21
	D_{mean}, Gy (SD)	29.4 (2.5)	27.1 (1.9)	26.9 (2.2)	0.10
ABM_{Atlas}	V_{10}, % (SD)	93.3 (2.6)	90.6 (4.3)	88.6 (4.8)	**<0.001**
	V_{20}, % (SD)	79.7 (6.1)	71.4 (7.2)	65.9 (5.1)	**<0.001**
	V_{30}, % (SD)	58.6 (6.6)	52.0 (6.1)	48.8 (4.9)	**<0.001**
	V_{40}, % (SD)	28.0 (5.4)	26.5 (5.1)	26.7 (5.2)	0.76
	D_{mean}, Gy (SD)	31.1 (1.7)	29.2 (2.0)	28.1 (1.7)	**<0.001**
Bowel	V_{30}, cc (SD)	515.0 (170.6)	539.4 (172.1)	551.5 (173.7)	**<0.01**
	V_{45}, cc SD)	146.6 (96.8)	154.9 (101.0)	157.9 (101.1)	**0.03**
	D_{max}, Gy (SD)	48.5 (1.5)	49.2 (1.6)	49.7 (1.8)	**<0.01**
Bladder	D_{max}, Gy (SD)	47.7 (1.1)	48.2 (1.0)	48.5 (1.3)	0.14
Rectum	D_{max}, Gy (SD)	47.2 (0.7)	47.7 (1.0)	47.9 (1.2)	0.21
PTV	V_{97}, % (SD)	99.2 (0.3)	98.9 (0.4)	98.6 (0.5)	**<0.001**
	D_{97}, Gy (SD)	44.6 (0.1)	44.6 (0.2)	44.5 (0.2)	**<0.01**
	V_{105}, % (SD)	28.7 (14.2)	37.7 (18.2)	40.1 (21.0)	0.07
	V_{110}, % (SD)	1.8 (5.9)	4.6 (9.5)	6.4 (11.3)	0.08

PBM, pelvic bone marrow; ABM, active bone marrow; PTV, planning target volume; SD, standard deviation. *: p-Value from two-sided paired t-test. Bold p-Value, statistically significant as $p < 0.05$.

tional imaging [15,24]. Collectively, these studies indicate the potential of preserving functional ABM as a strategy to reduce HT and improve chemotherapy tolerance.

This study has some limitations. First, the PET scans were performed at different institutions using different imaging platforms, potentially increasing variability. However, this would also provide a sense of variation that is likely to be encountered if atlas-based ABM-sparing approaches were applied in the population. Secondly, the Dice coefficient has limitations for the purposes of comparing "agreement" between volumes [26,27] and whether such agreement is high (based on the values we observed in this study) is open to some subjective interpretation. Nonetheless, we did observe a strong correlation between atlas and custom ABM volumes, lending to a straightforward interpretation of the Dice coefficient as the percentage of overlap between these two structures. Thirdly, the accuracy of the ABM atlas depends on the reliability of deformable image registration methods; thus spatial uncertainties could diminish the strength of the associations we observed.

A strength of our study was that we used a relatively large sample of 62 patients undergoing functional imaging, representing an international population treated on prospective clinical trials with rigorous quality assurance. This enabled us to use split-sample validation methods to determine whether the atlas-based model accurately represents the actual ABM distribution in an independent set of patients. Finally, we took the next step of conducting a treatment planning experiment to gauge what impact the implementation of atlas-based techniques might have in practice.

In summary, we found that atlas-based planning has the potential to obviate expensive functional imaging, at least for the purpose of reducing ABM dose, and is a promising treatment option

for underserved populations. However, further studies are needed to establish whether bone marrow-sparing techniques benefit patients.

Conflict of interest

None.

Acknowledgement

None.

References

[1] Keys HM et al. Cisplatin, radiation, and adjuvant hysterectomy compared with radiation and adjuvant hysterectomy for bulky stage IB cervical carcinoma. N Engl J Med 1999;340(15):1154–61.
[2] Rose PG et al. Concurrent cisplatin-based radiotherapy and chemotherapy for locally advanced cervical cancer. N Engl J Med 1999;340(15):1144–53.
[3] Das IJ. Intensity-modulated radiation therapy dose prescription, recording, and delivery: patterns of variability among institutions and treatment planning systems. J Natl Cancer Inst 2008:300–7. United States.
[4] Eifel PJ et al. Pelvic irradiation with concurrent chemotherapy versus pelvic and para-aortic irradiation for high-risk cervical cancer: an update of radiation therapy oncology group trial (RTOG) 90–01. J Clin Oncol 2004;22(5):872–80.
[5] Dueñas-González A. Phase III, open-label, randomized study comparing concurrent gemcitabine plus cisplatin and radiation followed by adjuvant gemcitabine and cisplatin versus concurrent cisplatin and radiation in patients with stage IIB to IVA carcinoma of the cervix. J Clin Oncol 2011. p. JCO. 2009.25. 9663.
[6] Green JA et al. Survival and recurrence after concomitant chemotherapy and radiotherapy for cancer of the uterine cervix: a systematic review and meta-analysis. Lancet 2001;358(9284):781–6.
[7] Torres MA et al. Comparison of treatment tolerance and outcomes in patients with cervical cancer treated with concurrent chemoradiotherapy in a prospective randomized trial or with standard treatment. Int J Radiat Oncol Biol Phys 2008;70(1):118–25.
[8] Abu-Rustum NR et al. Compliance with and acute hematologic toxic effects of chemoradiation in indigent women with cervical cancer. Gynecol Oncol 2001;81(1):88–91.
[9] Mell LK et al. Dosimetric predictors of acute hematologic toxicity in cervical cancer patients treated with concurrent cisplatin and intensity-modulated pelvic radiotherapy. Int J Radiat Oncol Biol Phys 2006;66(5):1356–65.
[10] Rose BS et al. Normal tissue complication probability modeling of acute hematologic toxicity in cervical cancer patients treated with chemoradiotherapy. Int J Radiat Oncol Biol Phys 2011;79(3):800–7.
[11] Mell LK et al. Dosimetric comparison of bone marrow-sparing intensity-modulated radiotherapy versus conventional techniques for treatment of cervical cancer. Int J Radiat Oncol Biol Phys 2008;71(5):1504–10.
[12] Lujan AE et al. Intensity-modulated radiotherapy as a means of reducing dose to bone marrow in gynecologic patients receiving whole pelvic radiotherapy. Int J Radiat Oncol Biol Phys 2003;57(2):516–21.
[13] Blebea JS et al. Structural and functional imaging of normal bone marrow and evaluation of its age-related changes. Seminars in nuclear medicine. Elsevier; 2007.
[14] Liang Y et al. Impact of bone marrow radiation dose on acute hematologic toxicity in cervical cancer: principal component analysis on high dimensional data. Int J Radiat Oncol Biol Phys 2010;78(3):912–9.
[15] Liang Y et al. Prospective study of functional bone marrow-sparing intensity modulated radiation therapy with concurrent chemotherapy for pelvic malignancies. Int J Radiat Oncol Biol Phys 2013;85(2):406–14.
[16] Rose BS et al. Correlation between radiation dose to 18 F-FDG-PET defined active bone marrow subregions and acute hematologic toxicity in cervical cancer patients treated with chemoradiotherapy. Int J Radiat Oncol Biol Phys 2012;83(4):1185–91.
[17] Elicin O et al. [18 F] FDG-PET standard uptake value as a metabolic predictor of bone marrow response to radiation: impact on acute and late hematological toxicity in cervical cancer patients treated with chemoradiation therapy. Int J Radiat Oncol Biol Phys 2014;90(5):1099–107.
[18] McGuire SM et al. A methodology for incorporating functional bone marrow sparing in IMRT planning for pelvic radiation therapy. Radiother Oncol 2011;99(1):49–54.
[19] Wyss JC et al. [18 F] Fluoro-2-deoxy-2-d-glucose versus 3′-deoxy-3′-[18 F] fluorothymidine for defining hematopoietically active pelvic bone marrow in gynecologic patients. Radiother Oncol 2015.
[20] McGuire SM et al. Spatial mapping of functional pelvic bone marrow using FLT PET. J Appl Clin Med Phys/Am Coll Med Phys 2014;15(4):4780.
[21] Li N et al. Validation of a knowledge-based automated planning system in cervical cancer as a clinical trial quality system. Int J Radiat Oncol Biol Phys 2015;93(3):S40.
[22] Li N et al. Highly efficient training, refinement, and validation of a knowledge-based planning quality-control system for radiation therapy clinical trials. Int J Radiat Oncol Biol Phys 2017;97(1):164–72.
[23] Albuquerque K et al. Radiation-related predictors of hematologic toxicity after concurrent chemoradiation for cervical cancer and implications for bone marrow-sparing pelvic IMRT. Int J Radiat Oncol Biol Phys 2011;79(4):1043–7.
[24] Rose BS et al. Correlation between radiation dose to (1)(8)F-FDG-PET defined active bone marrow subregions and acute hematologic toxicity in cervical cancer patients treated with chemoradiotherapy. Int J Radiat Oncol Biol Phys 2012;83(4):1185–91.
[25] Zhu H et al. Longitudinal study of acute haematologic toxicity in cervical cancer patients treated with chemoradiotherapy. J Med Imaging Radiat Oncol 2015;59(3):386–93 [quiz 394].
[26] Dice LR. Measures of the of ecologic association between species. Ecology 1945;26(3):297–302.
[27] Hanna GG, Hounsell AR, O'Sullivan JM. Geometrical analysis of radiotherapy target volume delineation: a systematic review of reported comparison methods. Clin Oncol (R Coll Radiol) 2010;22(7):515–25.